

Phase Transitions above the Yrast Line in ^{154}Dy

W. C. Ma,¹ V. Martin,² T. L. Khoo,³ T. Lauritsen,³ J. L. Egido,⁴ I. Ahmad,³ P. Bhattacharyya,⁵
M. P. Carpenter,³ P. J. Daly,⁵ Z. W. Grabowski,⁵ J. H. Hamilton,⁶ R. V. F. Janssens,³ D. Nisius,³ A. V. Ramayya,⁶
P. G. Varmette,¹ and C. T. Zhang⁵

¹Mississippi State University, Mississippi State, Mississippi 39762

²Análisis Numérico, Facultad de Informática, Universidad Politécnica de Madrid, E-28660 Madrid, Spain

³Argonne National Laboratory, Argonne, Illinois 60439

⁴Departamento de Física Teórica C-XI, Universidad Autónoma de Madrid, E-28049 Madrid, Spain

⁵Purdue University, West Lafayette, Indiana 47907

⁶Vanderbilt University, Nashville, Tennessee 37235

(Received 15 February 2000)

Spectra of the $E2$ quasicontinuum γ rays feeding different spin regions of the ^{154}Dy yrast line have been extracted. These are compared with corresponding theoretical spectra obtained by numerical simulations based on temperature-dependent Hartree-Fock theory, with thermal shape fluctuations. In this manner, different regions of the spin-energy plane can be examined. The results support the predictions of a smeared-out phase transition at high spin above the yrast line.

PACS numbers: 21.60.Jz, 23.20.-g, 24.60.Dr, 27.70.+q

Mean-field theory suggests [1–3] that nuclei can undergo phase transitions. An especially interesting example is the transitional nucleus ^{154}Dy , which is predicted [4] to change from a collective to an oblate aligned-particle structure with increasing spin and temperature, as sketched in Fig. 1. In a mesoscopic system, such as a nucleus, thermal shape fluctuations are expected to smear the phase transition and a question is whether remnant signatures of the phase transition persist at high excitation energies. A sudden change from collective to aligned-particle configurations at spin $34\hbar$ has indeed been confirmed along the zero-temperature yrast line in ^{154}Dy [5]. However, in excited states, where thermal fluctuations are dominant even at moderate temperature, it remains a challenge to obtain unambiguous signatures for a phase transition.

Calculations [6] based on results of mean-field theory and incorporating fluctuations have suggested that the quasicontinuum (QC) collective $E2$ spectrum can provide such a signature. Specifically, an $E2$ spectrum consisting of a unique two-peak feature was predicted [6] for ^{154}Dy , when the γ cascade straddles the two regions on either side of the phase-transition boundary. In contrast, only one broad QC peak is detected in the vast majority of nuclei [7]. This two-peak feature in the QC $E2$ spectrum has been, in fact, previously observed [8]. The calculations of Ref. [6] suggest that, while fluctuations indeed smear out the phase transition, they also play a critical role in providing an observable signature via the $E2$ spectrum. That is because no collective $E2$ spectrum would normally be expected in the oblate phase; it arises only because thermal fluctuations cause admixtures of collective (prolate and triaxial) shapes. This has been amply demonstrated in Ref. [6], where the calculated $E2$ spectra reproduce the different features observed [8,9] in $^{152,154,156}\text{Dy}$. A stringent test of the calculations consists of proving that the different $E2$ peaks indeed arise from the two phase regions, as will be

done in this paper. (Giant dipole resonances built on excited states provide another probe of hot rotating nuclei and their spectra are also affected by shape fluctuations; see, e.g., Refs. [3,10].)

The hot excited states in nuclei remain a little explored frontier since there are only a few experimental investigations of excited nuclear states above the yrast line, compared to studies of cold yrast states. This is partly because there has been no clearcut way to specify the spin-excitation energy being studied. In this Letter we propose

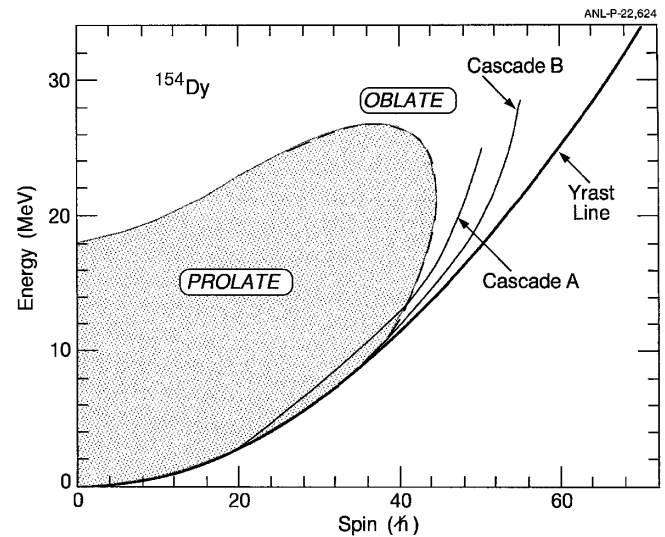


FIG. 1. Theoretical yrast line and regions of prolate (dotted) and oblate phases in ^{154}Dy . The phase boundary (dashed line) corresponds to the $\gamma = -60^\circ$ line in finite-temperature Hartree-Fock-Bogoliubov calculations without fluctuations [4]. Sketches of two cascade paths (A, B) are shown, which connect the experimental entry and exit points for cascades feeding into two selected regions of the yrast line, $I = (16-22)\hbar$ and $I = (34-36)\hbar$.

a new, but simple, way to provide this specification. By demanding that cascades feed the yrast line at a particular spin, the precursor QC spectrum then arises from states of higher spins. This can be simply accomplished by setting coincidence gates on specific yrast transitions. For example, cascade *A* in Fig. 1, which feeds into a low-spin region of the yrast line, can be selected; in this case we predict two *E2* peaks, one from each phase region. On the other hand, cascade *B*, selected by demanding entry into the yrast line at high spin, picks out cascades which traverse only the nominally oblate region; only the upper *E2* peak is then expected. Furthermore, the average initial point of the cascade is also deduced from the resulting QC spectrum. It is this knowledge of *both the initial and final points* that allows the decay pathways to be constrained. An alternative method is (i) to select the initial point by using measurements of multiplicity and sum energy and (ii) to determine the average point where the cascade enters the yrast line. Step (i) has been used before, see, e.g., Ref. [11], but without also requiring step (ii). The drawback with step (i), however, is that the achievable resolutions for multiplicity and sum energy are very coarse, typically $>25\%$ FWHM. A second critical requirement of our method is to directly compare, under *identical gating conditions*, the experimental and theoretical spectra, the latter obtained as described in Ref. [6].

The experiment was performed at the Lawrence Berkeley 88" Cyclotron. Excited states in ^{154}Dy were populated via the $^{36}\text{S}(^{122}\text{Sn}, 4n)$, reaction with a 165-MeV beam. The target consisted of a stack of three $350\ \mu\text{g}/\text{cm}^2$ self-supporting foils. The γ rays were detected with the early-implementation phase of the GAMMASPHERE spectrometer, which consisted of 36 Compton-suppressed Ge detectors at that time. A total of 1.3×10^9 events was collected, with a requirement of ≥ 3 suppressed Ge detectors in prompt coincidence.

Spectra were obtained for ^{154}Dy at three detector angles (forward, 90° , and backward), coincident with selected pairs of yrast transitions. This was achieved by constructing γ - γ matrices after coincidence gates were set on low-spin yrast transitions from $I^\pi = 2^+$ to 8^+ . Three matrices were constructed, where the x coordinate was the Ge-detector energy from detectors at any angle and the y coordinate was the energy from Ge detectors at three groups of angles: (a) 31.7° and 37.4° (10 detectors) with respect to the beam direction, (b) 90° (6 detectors), and (c) 162.7° , 148.3° , and 142.6° (15 detectors). Five 17.3° detectors were not used for the y coordinate because of stronger contamination from neutron-induced events in the forward angle. One-dimensional spectra were obtained from the γ - γ matrices by selecting energies on the x axis corresponding to yrast transitions of different spins. Several spectra originating from states with similar spins were summed to increase statistics.

Each spectrum was analyzed in the manner described in Ref. [9], with corrections for neutron interaction, coincidence summing, detector response (unfolding),

and photopeak efficiency, following the prescriptions of Refs. [12,13]. Discrete peaks (originating from the yrast region) were removed to obtain the QC portion of the γ -ray spectra (from excited states above the yrast region). Statistical γ rays were subtracted from fits to the high-energy tail of the spectra with the functional form $E_\gamma^3 \exp(-E_\gamma/T)$, where $T = 0.5$ MeV. Angular distribution coefficients (A_2, A_4) were extracted for each energy bin of the QC spectrum, by using the spectra at three different angles. The dipole and quadrupole components were then separated, based on the angular distribution coefficients. Each spectrum was normalized so that the ground-state transition has unit intensity; the integral then gives the multiplicity. From the multiplicity and average energy of each component, the total spins and energies removed by all γ rays entering each selected spin region could be deduced, with the assumption that $(0.5, 1.0, \text{ and } 2.0)\hbar$ angular momenta were removed by statistical, dipole, and quadrupole transitions, respectively. The average entry point for the total ^{154}Dy channel was thus found to be $56.1\hbar$ and 31 MeV. Table I summarizes the multiplicities for the *E2* QC components feeding different spin regions.

The spectra feeding the different regions of the yrast line are given in Fig. 2, where they are compared to equivalent theoretical spectra. A distinct and unusual feature is the occurrence of two broad peaks. The spectrum of *E2* transitions from excited states of a nucleus of approximately fixed deformation normally consists of a single broad peak [7], since the transition energy, $E_\gamma = (2I - 1)\hbar^2/J$, grows monotonically with spin I . (J is the moment of inertia.) Hence, the two-peak spectra provide a clear signal of a deviation from constant deformation.

To quantitatively understand the origin of the two peaks, we have performed theoretical calculations to simulate the QC decay of this nucleus by using a Monte Carlo method [6]. The collective *E2* strengths, which carry information about the structure and phase transition, are microscopically calculated as a function of spin I and excitation energy E from finite-temperature Hartree-Fock (FTHF) theory, with the standard set of pairing-plus-quadrupole force parameters and configuration space [14]. In order to reproduce the features of a finite system, we have to go beyond mean-field theory by including fluctuations in the shape degrees of freedom [4].

TABLE I. Theoretical and experimental quasicontinuum *E2* multiplicities for different gates. The numbers in the first row denote the selected initial spins of the gating transitions. The uncertainty in the experimental multiplicity is 10%, obtained by adding in quadrature the uncertainties in each step of the analysis.

Gates	2-10	12-14	16-24	26-32	34-38	40-46
Exp.	10.7	10.2	9.0	7.7	6.9	6.4
Theor.	9.8	9.8	9.2	7.3	5.9	4.6

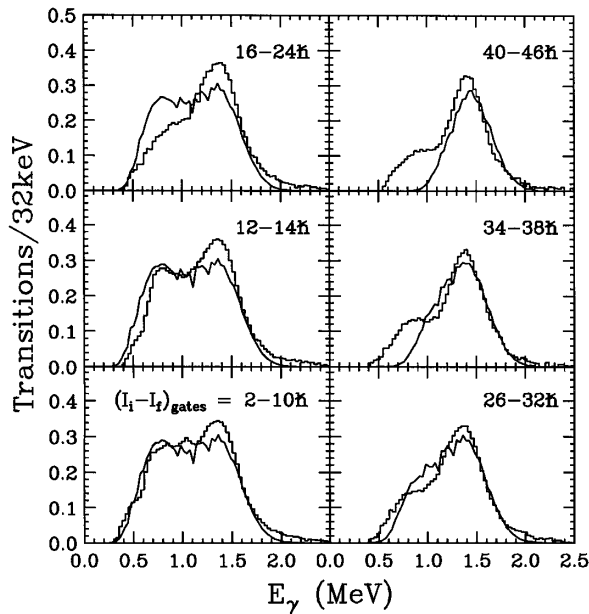


FIG. 2. Integral spectra of the quasicontinuum $E2$ transitions feeding into and above the indicated spin intervals. Histograms represent experimental results and solid lines represent the theoretical calculations. The labels $(I_i - I_f)_{\text{gates}}$ denote the spin interval of the transitions used for coincidence gates.

The probability of having a certain set of values, α , characterizing the deformation, is proportional to $e^{-F(\alpha;I,T)/T}$. $F(\alpha;I,T)$, the Landau free energy, is calculated at fixed α , I , and temperature T , by minimizing the corresponding grand canonical potential $\Omega = E - TS - \omega\sqrt{I(I+1)} - \lambda N - \alpha Q$. S is the entropy; the Lagrange multipliers ω , λ , and α are fixed to provide the right angular momentum I , particle number N , and multipole moment Q , respectively. In our case, α represents the β and γ deformation parameters. Hence, the probability of emitting a collective γ ray with the nucleus having a deformation parameter between α and $\alpha + d\alpha$ is given by

$$\frac{B(E2; \alpha, T; I \rightarrow I - 2)e^{-F(\alpha;I,T)/T} D[\alpha]}{\int e^{-F(\alpha;I,T)/T} D[\alpha]},$$

where $B(E2; \alpha, T; I \rightarrow I - 2)$ represents the reduced transition probability for a system with deformation α . The metric is given [15] by $D[\alpha] = \beta^4 |\sin 3\gamma| d\beta d\gamma$. This probability is then used in a Monte Carlo process to calculate the decay cascade, as described in Ref. [6].

The main characteristic of the calculation is that the number of adjustable parameters is kept to a minimum. The average entry spin and energy for the reaction are obtained directly from the experiment. The $E1$ -strength γ function has the standard giant dipole resonance (GDR) form [16], with a correction for the low-energy tail [17]. The input parameters are the energy at which the GDR peaks, chosen to be 14.96 MeV, and its width, 5 MeV. We also used a standard formula for the level density [18].

The γ cascade is followed until it reaches a specified energy, U_{cut} , above the yrast line; the reduced level den-

sity at lower energy will lead to discrete transitions. The procedure produces spectra that are equivalent to the experimental ones, where the discrete lines are removed. The cutoff is chosen to mimic the top of the pair gap; U_{cut} has a value of 1.5 MeV at $I = 0\hbar$ and linearly decreases to a value of 0.4 MeV for $I = 30\hbar$, remaining constant thereafter.

Figure 2 shows the experimental and theoretical QC $E2$ spectra from coincidence gates from different spin regions. The spectra are normalized such that the area under each spectrum gives the total multiplicity of the associated γ rays. As can be seen in Table I, when the gating spin increases, the QC $E2$ multiplicity decreases. In the low-spin region, an almost constant $E2$ multiplicity was obtained since most feeding cascades have already entered the yrast line at higher spins. In the high-spin region the QC $E2$ multiplicity decreases since the cascades are shorter as they are “forced” into the yrast line at higher spin. Two peaks, centered around 0.8 and 1.4 MeV, are prominent in the spectra from low-spin gates, as found in a previous study [8]. Since the lowest gate, $(2-10)\hbar$ (see Fig. 2), collects all of the cascades, this spectrum is similar to that in Fig. 2(a) of Ref. [8], which was obtained under similar conditions. (Small differences may be attributed to differences in the beam energy.)

The two-peak feature indicates a redistribution of γ -ray energies along the deexcitation pathways. In the later decay stages, when the cascades approach the yrast line at medium and low spins, the moment of inertia increases and transition energies shift downwards, causing the clustering around 800 keV and the dip around 1.1 MeV. In the spectra gated at higher spins, contributions of cascades traversing the low-spin prolate region of the I - E plane are eliminated, thus reducing the strength of the low-energy component. This demonstrates that the low-energy component originates mainly from regions of lower spins. The high-energy peak begins to dominate over the low-energy peak for cascades feeding regions as low as $(16-24)\hbar$ and, in the theoretical spectra, becomes almost the only component for feeding above $32\hbar$. This clearly identifies the region $I > 32\hbar$ as the one with the smaller average moment of inertia.

In the experimental spectra, the low-energy component does not disappear completely, probably reflecting larger fluctuations than are present in the theory. It remains to be seen whether additional fluctuations can be introduced by inclusion of pairing or of superdeformed shapes found [19] in this nucleus. Further calculations will be necessary with more realistic forces, such as the Gogny interaction, which is capable of describing superdeformation and which includes pairing.

The spectra in Fig. 2 might be termed integral spectra. Each spectrum, which is obtained from coincidence gates on yrast transitions of specific spin, selects all QC cascades that feed into the yrast line above that spin. As the spin threshold increases, the QC pathways become more narrowly defined in spin, thus better specifying the I - E region

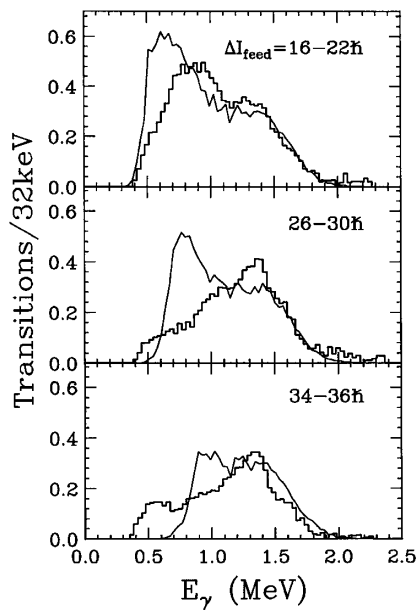


FIG. 3. Differential $E2$ spectra feeding into the yrast line *only* in the indicated spin region ΔI_{feed} . Histograms and solid lines correspond to experiment and theory. The approximate decay pathways corresponding to the top and the bottom spectra are shown as cascades A and B , respectively, in Fig. 1.

being studied. However, as the threshold spin is lowered, the selectivity of such integral spectra decreases since all contributions from higher spins persist. It is possible to emphasize the particular QC cascades from a lower-spin region, by using differential spectra that feed *only* a narrow spin interval. For example, the QC spectrum feeding into the yrast states with only $I = (16-22)\hbar$ can be extracted by subtracting the spectra gated on the transitions depopulating the 16^+ and 24^+ levels (after correct normalization); see Fig. 3. (The result is reliable only when the γ intensities and the differences are large.) The low-energy $E2$ component is now significantly stronger than in the integral $I = (16-24)\hbar$ spectrum (Fig. 2). Again this emphasizes that this component must arise from the low-spin region. In contrast, in the differential spectrum feeding the spin interval $(26-30)\hbar$, this low-energy component is markedly smaller, indicating that the γ cascade crosses the phase-transition boundary around spin $(34-36)\hbar$. Although the trend of a low-energy component that diminishes with yrast entry spin is reproduced by theory, discrepancies in details indicate that the theoretical phase boundary is at higher spin than found in the experiment, so that the γ cascade crosses it at $I \sim 40\hbar$; see also Fig. 1.

In conclusion, *both* experimental and theoretical quasicontinuum spectra exhibit two broad peaks, with pronounced changes in relative strengths when going from low- to high-spin gates. The varying strengths provide an incisive probe of the change in nuclear structure in the two zones of the I - E plane. The low-energy $E2$ component originates from the lower spin region, with prolate deformation. The high-energy component is largely from the nominally oblate region of the phase diagram, where strong fluctuations give rise to $E2$ transitions. Despite the fluctuations present in a finite system, signatures of a phase transition are seen to clearly persist in both the experimental and theoretical spectra.

This work was partly supported by U.S. DOE Grants No. DE-FG02-95ER40939, No. W-31-109-ENG-38, No. DE-FG02-87ER40346, and No. DE-FG05-88ER40407. Work at Madrid was supported by DGICyT, Spain, under project PB97-0023. Part of the numerical calculations was done at the CTP, Universidad Politecnica de Madrid. W.C.M and V.M. thank Argonne for partial support during their visits; V.M. also acknowledges the support of the Vicerrectorado de Investigacion of the UPM.

- [1] J.L. Egido *et al.*, Phys. Lett. B **178**, 139 (1986).
- [2] A.L. Goodman, Phys. Rev. C **39**, 2478 (1989).
- [3] Y. Alhassid, B. Bush, and S. Levit, Phys. Rev. Lett. **61**, 1926 (1988); Y. Alhassid and B. Bush, Nucl. Phys. **A509**, 461 (1990).
- [4] V. Martin and J.L. Egido, Phys. Rev. C **51**, 3084 (1995).
- [5] W.C. Ma *et al.*, Phys. Rev. Lett. **61**, 46 (1988).
- [6] V. Martin *et al.*, Phys. Rev. C **51**, 3096 (1995).
- [7] R.M. Diamond and F.S. Stephens, Annu. Rev. Nucl. Part. Sci. **30**, 85 (1980).
- [8] R. Holzmann *et al.*, Phys. Rev. Lett. **62**, 520 (1989).
- [9] R. Holzmann *et al.*, Phys. Lett. B **195**, 321 (1987).
- [10] M. Gallardo *et al.*, Nucl. Phys. **A443**, 415 (1985).
- [11] C. Baktash *et al.*, Nucl. Phys. **A520**, 555c (1990).
- [12] R. Holzmann *et al.*, Nucl. Instrum. Methods Phys. Res., Sect. A **260**, 153 (1987).
- [13] D.C. Radford *et al.*, Nucl. Instrum. Methods Phys. Res., Sect. A **258**, 111 (1987).
- [14] K. Kumar and M. Baranger, Nucl. Phys. **A110**, 529 (1968).
- [15] Y. Alhassid, Nucl. Phys. **A553**, 137c (1993).
- [16] G.A. Bartholomew *et al.*, Adv. Nucl. Phys. **17**, 229 (1973).
- [17] S.G. Kadenskii *et al.*, Sov. J. Nucl. Phys. **37**, 165 (1983); C.M. McCullagh *et al.*, Phys. Rev. C **23**, 1394 (1981).
- [18] D.W. Lang, Nucl. Phys. **77**, 545 (1966).
- [19] D. Nisius *et al.*, Phys. Rev. C **51**, R1061 (1995).